Highly reproducible, hysteresis-free, flexible strain sensors by inkjet printing of carbon nanotubes

Fulvio Michelis[1,2], Laurence Bodelot[3], Yvan Bonnassieux[2], Bérengère Lebental[1,2]*

[1] Université Paris-Est, IFSTTAR, COSYS/LISIS, Paris, France

[2] Laboratoire de Physique des Interfaces et Couches Minces (LPICM), UMR 7647, Ecole Polytechnique-CNRS, Palaiseau, France

[3] Laboratoire de Mécanique des Solides (LMS), UMR 7649, Ecole Polytechnique-CNRS, Palaiseau, France

Supplementary information

1. *Literature review on CNN sensors*

Table 1 and its references [1] to [35] present the state of the art regarding to CNN-based sensors on substrates. It excludes papers on freestanding CNN and on CNT composites. It includes references on both rigid and flexible substrates. References are classified by observables, fabrication method, substrates and by whether they provide insight into variability (in the fabrication process and in the device sensitivity).

We observe here that while the variability on the fabrication process is frequently studied (11 over 35), very few references (only 7 over the 35 reported here) address the issue of variability on device sensitivity. The studies that address it compare only the sensitivity of very few devices (up to 4) and provide no satisfying analysis of standard deviation on the sensitivity. This appears to be true for all type of sensors reported to this day, both on rigid and flexible substrates, either for mechanical, chemical (gas and liquid phase) or light sensing.

Ref	**Observables**	**Year**	**Fabrication**	**Substrate**	**Device-to-device variability on fabrication**	**Device-to-device variability on sensitivity**
Inkjet-printed sensors with study of variability						
[1]	Strain	2012	Ink-jet printing	PET	3 set of 3 sensors compared Best std dev 3.5%	No
[2]	Gas (NO_2, CO)	2009	Ink-jet printing	4in. Si/SiO_2 wafer	6 sensors compared No std dev provided Std dev<4%	4 sensors compared No std dev provided

* Corresponding author. Tel: +33 1 81 66 81 18. E-mail: berengere.lebental@ifsttar.fr (Bérengère Lebental)

[3]	pH	2009	Ink-jet printing	glass	5.6% over 10 sensors	No
[4]	Anti-oxydant power	2014	Inkjet printing	Kapton polyimide	Overlaid plots of amperometric response for batches of 6 and 4 sensors Std dev : 7% and 20% on the two parameters extracted from amperometric response	Two sets of two devices compared
Inkjet printing with study of variability						
[5]	Strain	2012	Inkjet printing	PDMS	No	No
[6]	Relative humidity	2013	Inkjet printing	Kapton polyimide	No	No
[7]	Gas (CO2)	2013	Inkjet printing	Flexible laminate	No	No
[8]	Gas (Ammonia)	2012	Inkjet printing	Paper	No	No
[9]	Electrochemical sensor	2013	Ink-jet printing	PVP	No	No
[10]	Light	2014	Inkjet printing	Si/SiO2	No	No
[11]	Infrared	2011	Inkjet printing	Kapton Polyimide	No	No
Other liquid phase based approach Insight into variability						
[12]	Chemical (Hg2+ and NH4+)	2011	Self assembly	Si/SiO2	Dispersion plot provided. 21 sensors. Conductance range spanning 2 orders of magnitude	Dispersion plot provided. 21 sensors. Sensitivity range spanning 2 orders of magnitude
[13]	Gas (NO2; nitrotoluene)	2003	Drop casting	Si/SO2	Yes	3 devices compared 7% variability on

						the slope (DY/DX) 25% variability on the Y-intercept
[14]	Gas	2010	Vacuum filtration and transfer	Si/SiO2	Yes (Resistances of 23 devices provided)	No
[15]	Relative humidity	2012	Spray-coating	PPE	3 resistance values provided (160% std dev)	No
[16]	Strain	2007	Direct drying	Epoxy over Steel	Range of resistances provided	No
Other liquid phase based approach- Strain sensors No insight into variability						
[17]	Strain	2012	Filtration and contact transfer	SiO2	No	No
[18]	Strain	2010	Vacuum filtration and transfer	PDMS	No	No
[19]	Strain	2004	Filtration and drying	PVC on brass	No	No
[20]	Strain	2008	Filtration	Aluminium	No	No
[21]	Strain Pressure	2011	Spray coating	PDMS	No	No
Other liquid phase based approach – Chemical sensors No insight into variability						
[22]	Relative humidity	2012	Spray coating	PET	No	No
[23]	Humidity	2009	Dielectrophoresis	Si/SiO2	No	No
[24]	Gas (O2)	2012	Drop casting Self assembly	Glass	No	No

[25]	Gas (H2)	2014	Drop casting	Glass	No	No
[26]	Gas (H2)	2012	Aerosol-jet printing	Si/SiO_2	No	No
[27]	Gas (Ammonia)	2014	Drop casting	Kapton Polyimide	No	No
[28]	Gas (Ammonia)	2014	Drop casting	Unspecified plastics	No	No
[29]	Gas (Ammonia)	2013	Paint brush	Cotton	No	No
[30]	Gas (NO2, NH3, EtOH and acetone)	2014	Screen printer	Alumina	No	No
[31]	Water	2013	Direct casting	Glass	No	No
Methods based on mechanical compression to form films						
[32]	Strain	2012	Press-tablets	PMMA	Range of resistance between 6 and 9 (std dev<25%)	Gauge factor for 2 sensors provided (GF=60 ; 70) (std dev 11%)
[33]	Gas	2013	Pellet compression	Paper	Yes	Comparison between 3 devices displayed but no std deviation provided
Methods based on direct growth (with or without transfer)						
[34]	Chemical (Dopamine)	2013	Direct growth	Si/SO2	No	No
[35]	Strain	2011	Direct growth and transfer	PDMS	No	3 devices compared. Strong device to device differences

Table 1 : Literature review on CNN sensors and their variability

[1] A. Benchirouf, E. Sowade, A. Al-Hamry, T. Blaudeck, O. Kanoun and R. Baumann, "Investigation of RFID passive strain sensors based on carbon nanotubes using inkjet printing technology," in *9th IEEE Int. Multiconference on Systems, Signals and Devices*, 2012.

[2] J. Kim, J.-H. Yun, J.-W. Song and C.-S. Han, "The spontaneous metal-sitting structure on carbon nanotube arrays positioned by inkjet printing for wafer-scale production of high sensitive gas sensor units," *Sensors and Actuators B: Chemical,* vol. 135, pp. 587-591, 2009.

[3] M. O'Toole, R. Shepherd, G. G.Wallace and D. Diamond, "Inkjet printed LED based pH chemical sensor for gas sensing," *Analytica Chimica Acta,* vol. 652, pp. 308-314, 2009.

[4] A. Lesch, F. Cortés-Salazar, M. Prudent, J. Delobel, S. Rastgar, N. Lion, J.-D. Tissot, P. Tacchini and H. H. Girault, "Large scale inkjet-printing of carbon nanotubes electrodes for antioxidant assays in blood bags," *Journal of Electroanalytical Chemistry,* Vols. 717-718, pp. 61-68, 2014.

[5] T. Kim, J. Byun, H. Song and Y. Hong, "Inkjet-printed SWCNT films for stretchable electrode and strain sensor applications," in *IEEE 70th Annual Device Research Conference (DRC)*, University Park, TX, USA, 2012.

[6] Y. Feng, L. Xie, M. Mäntysalo, Q. Chen and L.-R. Zheng, "Electrical and humidity-sensing characterization of inkjet-printed multi-walled carbon nanotubes for smart packaging," in *IEEE Sensors*, Baltimore, MD, USA, 2013.

[7] A. Vena, L. Sydänheimo, M. M. Tentzeris and L. Ukkonen, "A Novel Inkjet Printed Carbon Nanotube-Based Chipless RFID Sensor for Gas Detection," in *43rd European Microwave Conference*, Nuremberg, Germany, 2013.

[8] H. Lee, G. Shaker, V. Lakafosis, R. Vyas, T. Thai, S. Kim and X. Yi, "Antenna-based "Smart Skin" Sensors for Sustainable, Wireless Sensor Networks," in *IEEE ICIT*, 2012.

[9] R. P. Tortorich, E. Song and a. J.-W. Choi, "Inkjet-Printed Carbon Nanotube Electrodes for Electrochemical Sensor Applications," in *224th ECS Meeting*, 2013.

[10] E. Katzir, S. Yochelis, Y. Paltiel, S. Azoubel, A. Shimoni and S. Magdassi, "Tunable inkjet printed hybrid carbon nanotubes/nanocrystals light sensor," *Sensors and Actuators B: Chemical,* vol. 196, pp. 112-116, 2014.

[11] A. Gohier, A. Dhar, L. Gorintin, P. Bondavalli, Y. Bonnassieux and C. Cojocaru, "All-printed infrared sensor based on multiwalled carbon nanotubes," *Applied Physics Letters,* vol. 98, p. 063103, 2011.

[12] B. Y. Lee, M. G. Sung, J. Lee, K. Y. Baik, Y.-K. Kwon, M.-S. Lee and S. Hong, "Universal Parameters for Carbon Nanotube Network-Based Sensors: Can Nanotube Sensors Be Reproducible?," *ACS Nano,* vol. 5, pp. 4373-4379, 2011.

[13] J. Li, Y. Lu, Q. Ye, M. Cinke, J. Han and M. Meyyappan, "Carbon Nanotube Sensors for Gas and Organic Vapor Detection," *Nano Letters,* vol. 3, pp. 929-933, 2003.

[14] C. R. Field, J. Yeom, A. Salehi-Khojin and R. I. Masel, "Robust fabrication of selective and reversible polymer coated carbon nanotube-based gas sensors," *Sensors and Actuators B:*

Chemical, vol. 148, pp. 315-322, 2010.

[15] Y. Feng, A. L. Cabezas, Q. Chen, L.-R. Zheng and Z.-B. Zhang, "Flexible UHF Resistive Humidity Sensors Based on Carbon Nanotubes," *IEEE Sensors Journal,* vol. 12, pp. 2844-2950, 2012.

[16] C. Cao, C. Hu, Y. Xiong, X. Han, Y. Xi and J. Miao, "Temperature dependent piezoresistive effect of multi-walled," *Diamond and Related materials,* vol. 16, pp. 388-392, 2007.

[17] D. J. Cohen, D. Mitra, K. Peterson and M. M. Maharbiz, "A Highly Elastic, Capacitive Strain Gauge Based on Percolating Nanotube Networks," *Nano Letters,* vol. 12, pp. 1821-1825, 2012.

[18] "Carbon nanotube film piezoresistors embedded in polymer membranes," *Applied Physics Letters,* vol. 96, p. 013511, 2010.

[19] P. Dharap, Z. Li and S. Nagarajaiah, "Nanotube film based on single-wall carbon nanotubes for strain sensing," *Nanotechnology,* vol. 15, pp. 379-382, 2004.

[20] X. Li, C. Levy and L. Elaadil, "Multiwalled carbon nanotube film for strain sensing," *Nanotechnology,* vol. 19, p. 045501, 2008.

[21] D. J. Lipomi, M. Vosgueritchian, B. C.-K. Tee, S. L. Hellstrom, J. A. Lee, C. H. Fox and a. Z. Bao, "Skin-like pressure and strain sensors based on transparent elastic films of carbon nanotubes," *Nature Nanotechnology,* vol. 6, pp. 788-792, 2011.

[22] V. Scardaci, R. Coull, J. N. Coleman, L. Byrne and G. Scott, "Carbon nanotube network based sensors," in *12th IEEE Intl Conference on Nanotechnology*, Birmingham, UK, 2012.

[23] L. Liu, X. Ye, K. Wu, R. Han, Z. Zhou and a. T. Cui, "Humidity Sensitivity of Multi-Walled Carbon Nanotube Networks Deposited by Dielectrophoresis," *Sensors,* vol. 9, pp. 1714-1721, 2009.

[24] C. Cava, R. Salvatierra, D. Alves, A. Ferlauto, A. Zarbin and L. S. Roman, "Self-assembled films of multi-wall carbon nanotubes used in gas sensors to increase the sensitivity limit for oxygen detection," *Carbon,* vol. 50, pp. 1953-1958, 2012.

[25] J. Garcia-Aguilar, I. Miguel-Garcıa, A. Berenguer-Murcia and D. Cazorla-Amoros, "Single wall carbon nanotubes loaded with Pd and NiPd nanoparticles for H2 sensing at room temperature," *Carbon,* vol. 66, pp. 599-611, 2014.

[26] R. Liu, H. Ding, J. Lin, F. Shen, Z. Cui and T. ZHang, "Fabrication of platinum-decorated single-walled carbon nanotube based hydrogen sensors by aerosol jet printing," *Nanotechnology,* vol. 23, p. 505301, 2012.

[27] Y. Ling, H. Zhang, G. Gu, X. Lu, V. Kayastha, C. S. Jones, W.-S. Shih and D. C. Janzen, "A Printable CNT-Based FM Passive Wireless Sensor Tag on a Flexible Substrate With Enhanced Sensitivity," *IEEE Sensors journal,* vol. 14, pp. 1193 - 1197, 2014.

[28] F. Rigoni, G. Drera, S. Pagliara and A. Goldoni, "High sensitivity, moisture selective, ammonia gas sensors based on single-walled carbon nanotubes functionalized with indium tin oxide nanoparticles," *Carbon ,* vol. 80, pp. 356-363, 2014.

[29] J.-W. Han, B. Kim, J. L and M. Meyyappan, "A carbon nanotube based ammonia sensor on cotton

textile," *Applied Physics Letters,* vol. 102, p. 193104, 2013.

[30] G. P. Evans, D. J. Buckley, N. T. Skipper and I. P. Parkin, "Single-walled carbon nanotube composite inks for printed gas sensors: enhanced detection of NO2, NH3, EtOH and acetone," *RCS Advanced,* vol. 4, pp. 51395-51403, 2014.

[31] H. Qi, E. Mäder and J. Liu, "Unique water sensors based on carbon nanotube–cellulose composites," *Sensors and Actuators B: Chemical,* vol. 185, pp. 225-230, 2013.

[32] K. S. Karimov, F. A. Khalid and M. T. S. Chani, "Carbon nanotubes based strain sensors," *Measurement,* vol. 45, pp. 918-921, 2012.

[33] K. A. Mirica, J. M. Azzarelli, J. G. Weis, J. M. Schnorr and T. M. Swager, "Rapid prototyping of carbon-based chemiresistive gas sensors on paper," *PNAS,* pp. 3265-3270, 2013.

[34] S. Sansuk, E. Bitziou, M. B. Joseph, J. A. Covington and M. G. Boutelle, "Ultrasensitive Detection of Dopamine Using a Carbon Nanotube," *Analytical chemistry,* vol. 85, pp. 163-169, 2013.

[35] T. Yamada, Y. Hayamizu, Y. Yamamoto, Y. Yomogida, A. Izadi-Najafabadi, D. N. Futaba and K. Hata, "A stretchable carbon nanotube strain sensor for human-motion detection," *Nature Nanotechnology,* vol. 6, pp. 296-301, 2011.

2. *Roughness calculation*

The roughness was calculated as the standard deviation of the profile height to the average height, according to the Root Mean Square formula:

$$R_{RMS} = \sqrt{\frac{1}{n}\sum_{i=1}^{n}(h_i - h_{mean})^2}$$

3. *Ink optimization*

Even though the dichlorobenzene-based ink is printable without added surfactant, we observed a poor homogeneity of the deposition as well as a pronounced coffee-ring effect (Figure 1a). The use of SDBS as surfactant is known to increase the ink wettability [36]. Added to the dichlorobenzene-based ink, the resulting printed layer is continuous and highly uniform (Figure 1b).

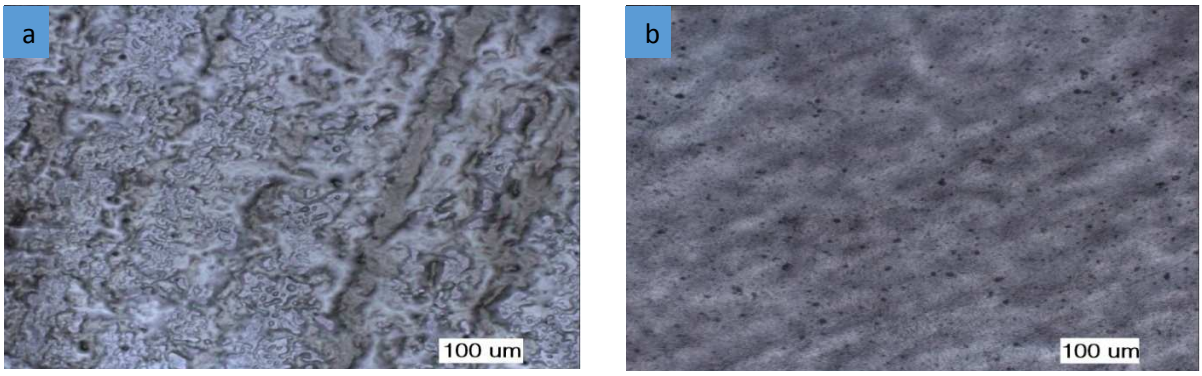

Figure 1: a) 20-layer deposition with no SDBS addition in the ink. The deposition is not uniform on the substrate. b) 20-layer deposition with use of SDBS as surfactant in the ink. The deposition is uniform.

4. *Rinsing process*

Figure 2: Effect of rinsing on the CNN at the micro scale. a-b) SEM image of a single layer deposition a) before rinsing. b) after rinsing. Most traces of surfactant and solvent have been removed. c) Resistance of a 20-layer deposition depending on the frequency of the rinsing step. Rinsing every two layers instead of every layer does not increase resistance significantly, but decreases the fabrication time considerably. A process based on rinsing every two layers was thus selected.

a shows a single CNT layer without application of the rinsing process. Even though it appears continuous under optical microscopy, it is poorly conducting (resistance above 1 GΩ), due to the presence of leftover SDBS particles as well as dichlorobenzene clearly observed on SEM images.

The rinsing process consists of immersion and slight agitation of the sample in methanol and acetone for 8 second followed by drying under nitrogen flow. This process removes most leftover surfactant and solvent (Figure 2: Effect of rinsing on the CNN at the micro scale. a-b) SEM image of a single layer deposition a) before rinsing. b) after rinsing. Most traces of surfactant and solvent have been removed. c) Resistance of a 20-layer deposition depending on the frequency of the rinsing step.

Rinsing every two layers instead of every layer does not increase resistance significantly, but decreases the fabrication time considerably. A process based on rinsing every two layers was thus selected.

b), though some traces of solvent can still be observed. Decrease of the resistance by several orders of magnitude is directly observed.

The lowest deposition resistance is observed when the CNT film is rinsed after each deposited layer. However, this process is very time consuming. To identify the optimal rinsing frequency, we measured the resistance of a 20-layer film depending on the frequency of the rinsing step. We found out that rinsing every two layers is the best compromise (Figure 2: Effect of rinsing on the CNN at the micro scale. a-b) SEM image of a single layer deposition a) before rinsing. b) after rinsing. Most traces of surfactant and solvent have been removed. c) Resistance of a 20-layer deposition depending on the frequency of the rinsing step. Rinsing every two layers instead of every layer does not increase resistance significantly, but decreases the fabrication time considerably. A process based on rinsing every two layers was thus selected.

c).

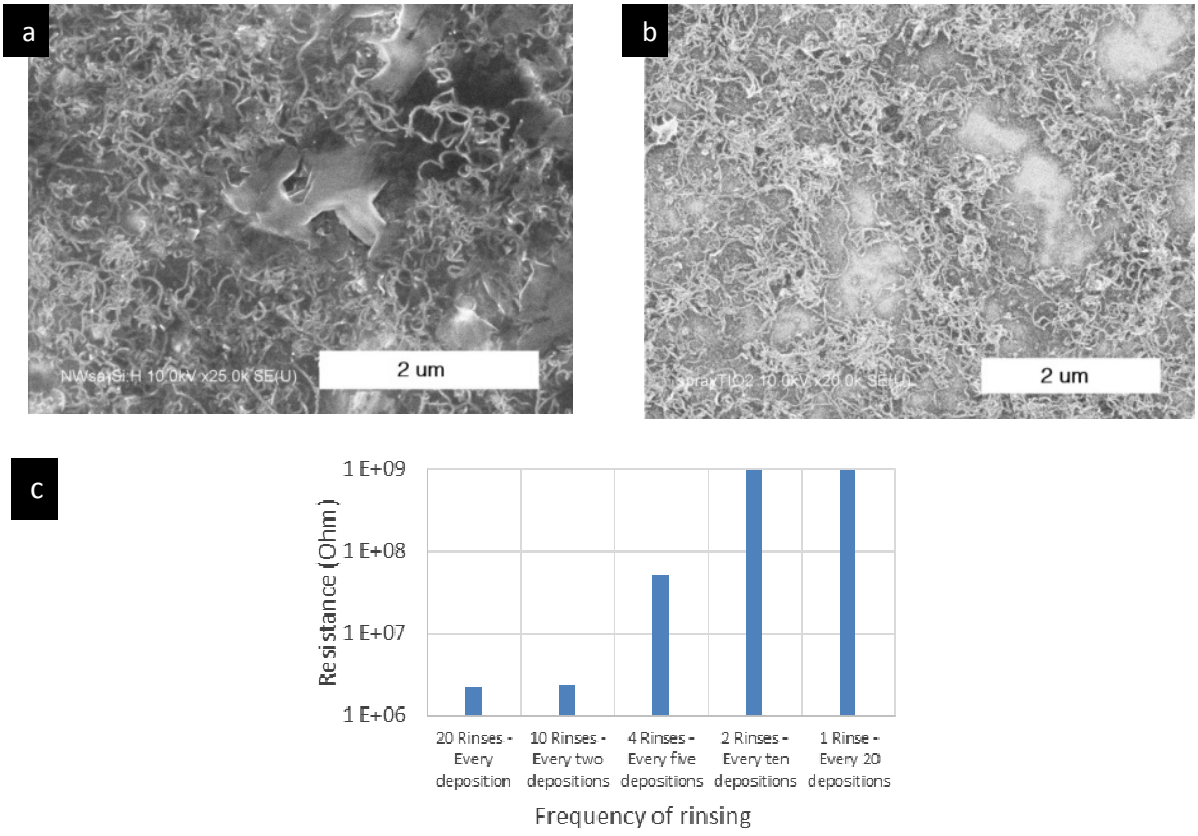

Figure 2: Effect of rinsing on the CNN at the micro scale. a-b) SEM image of a single layer deposition a) before rinsing. b) after rinsing. Most traces of surfactant and solvent have been removed. c) Resistance of a 20-layer deposition depending on the frequency of the rinsing step. Rinsing every two layers instead of every layer does not increase resistance significantly, but decreases the fabrication time considerably. A process based on rinsing every two layers was thus selected.

5. *Nanotube density estimation*

Figure 3 shows a typical image used to estimate manually the number of CNT by unit area. On the following image (size approx 5µmx3.5µm), the count reached 250CNT/µm². A downward bias is expected, as despite the high resolution imaging, the number of CNT in very dense cluster remains difficult to assess.

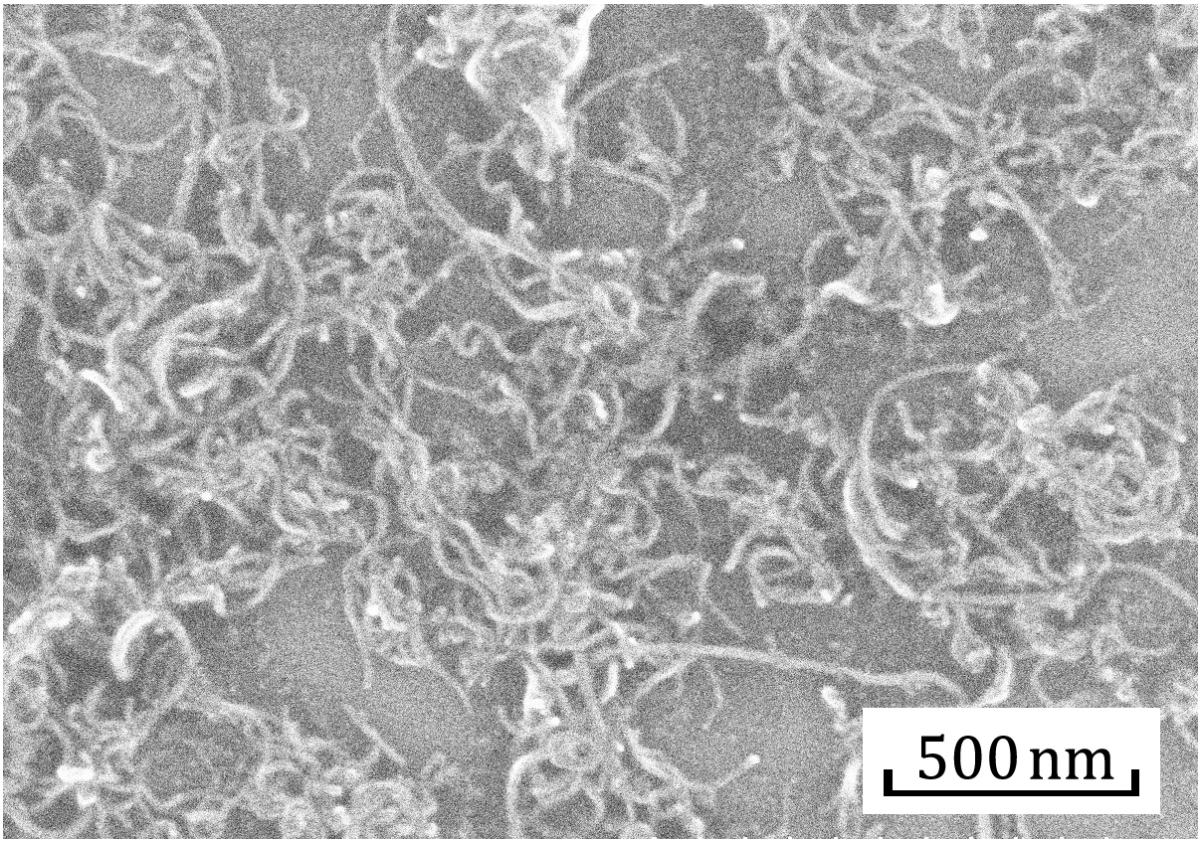

Figure 3 Image used for the estimation of the CNT surface density.

6. *Standard deviations measured on different batches of devices*

Table 2 summarizes the batches considered here.

Batch number	Number of devices in batch	Average resistance	Standard deviation on resistance	Comment
1	4	632kΩ	8.4%	Best standard deviation
2	5	461kΩ	18%	
3	3	252kΩ	18%	
4	8	156kΩ	15%	Lowest resistance Batch used for subsequent mechanical characterization
5	72	3.6MΩ	43%	23 sensors over 72 were characterized Process yield: 91% The resistance and standard deviation of this large batch is higher, due to unexpected lower thickness and lower homogenetity of the gold evaporation process.

Table 2: Summary of considered batches

7. *Mechanical properties of the ETFE substrate*

Figures 4a and 4b shows the force-strain response of the substrate for a 8N load, corresponding to 4000με, with 5 min periodicity.

Overall, the substrate force/strain response remains linear, but the substrate undergoes a slight creep during load cycles, approx 27με by cycle (0.6% of the max strain) for a 8N load cycle with 5min periodicity. The creep effect increases with both load and load rate.

Based on measuring the time delay between stress and strain curves during load cycles, the response time of the films here is found to range between 0,1s and 3s for load rates between 0.05N/s and 0.1N/s. There is no clear trend between load rates and response time, as the response time includes the response time of the glued clamps, which is not negligible with respect to the overall response time.

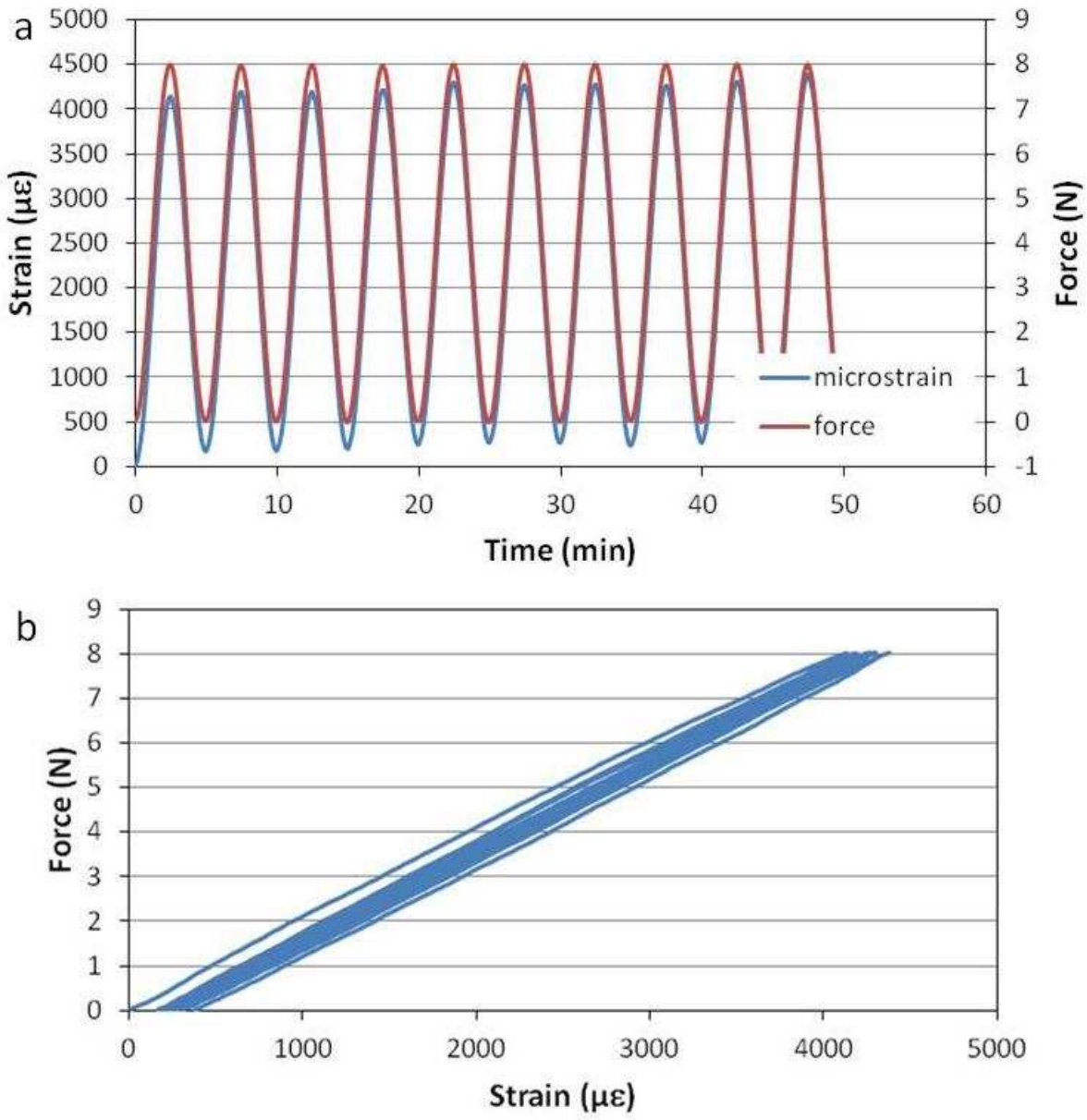

Figure 4: a) Strain-stress-time plots during 4N cyclic loads b) Corresponding force-strain plot showing the onset of creep

8. *Insight into modeling of the CNN network*

The modeling of the CNN network fabricated here is described in details in F. Michelis PhD thesis, to be available online by October 2015. Briefly, CNT are modeled as soft-cored objects, either straight or wavy. The model accounts for a statistical distribution of CNT diameter, length and waviness parameters. The parameters of the statistical distribution are extracted for SEM images of the deposition. The method relies on creating a statistical distribution of CNT in 3D by successive deposition of 2D layers, according to the layer by layer fabrication method.

An algorithm provides the number of contacts with respect to the parameters of the model and to the strains applied to the volume of study. Previous works in the state of the art show that the variation of resistance in the domain is proportional to the variation of the number of contacts.

Among others, the results are as follows:

- The standard deviation on the gauge factor is much lower for CNN further from the percolation threshold (figure 5a)
- Accounting for CNT waviness yields a quadratic dependence at large strains between number of contacts and strain, which cannot be reproduced with straight CNT only (figure 5b).

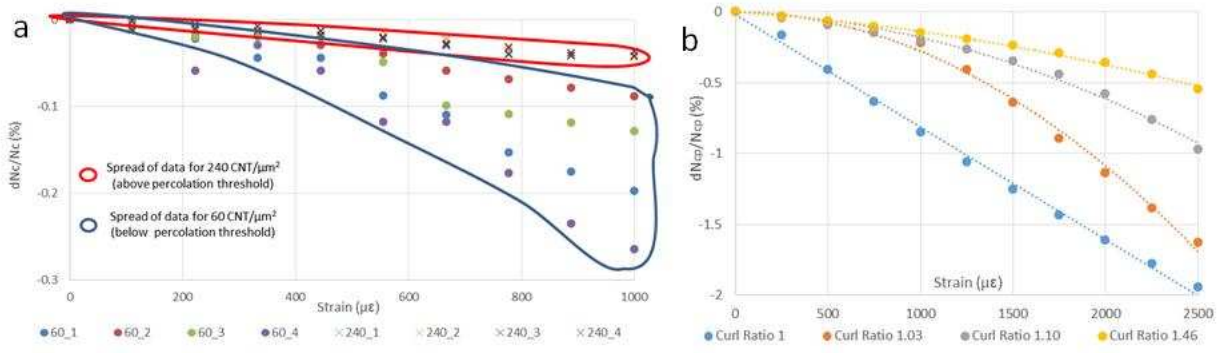

Figure 5. a) Variability on the strain sensitivity close to and far from the percolation threshold. b) Strain sensitivity for straight CNT (curl ratio=1) and for wavy CNT. The strain sensitivity is non linear for non-straight CNT, as observed experimentally.

9. *Hysteresis at large strain*

Figures 6a) and 6b) display the resistance/strain curves for cyclic loading of resp. 4N and 8N with periodicity resp. 10s and 5min. Corresponding maximum strain are resp. 2500με and 4000με, so are beyond the linear range of the devices. Expectedly, the response is hysteretic, the surface of the hysteresis increasing with maximum strain. Both curves display creep in strain and in resistance, the creep in strain being more intense at 4N because the load rate is much faster, the creep in resistance being more for 8N because the irreversibility in the network is more pronounced.

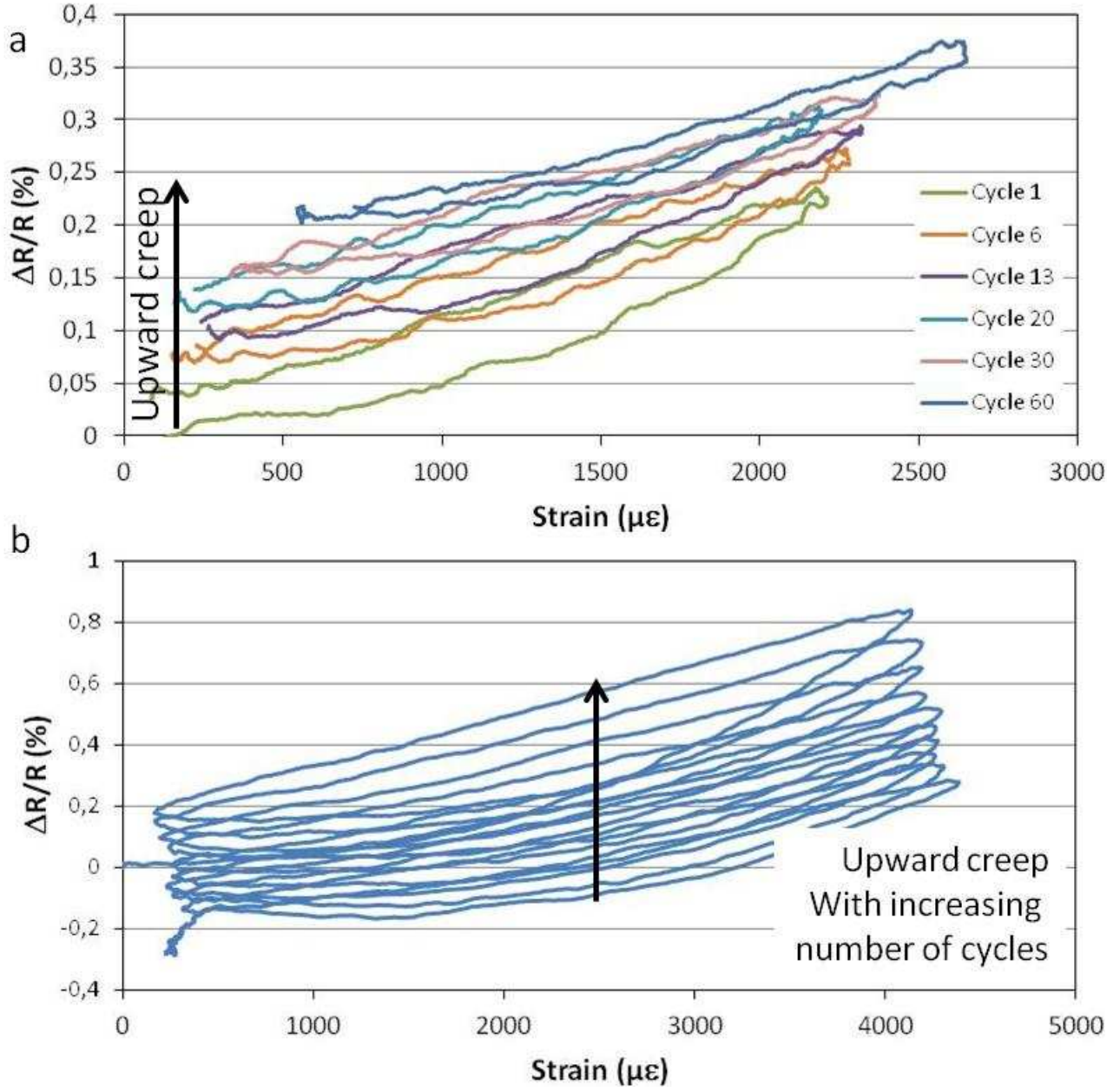

Figure 6: Resistance-strain curves during high strain load cycles: a) 4N, 2500∝ε, 10s period ; b) 8N, 4000με, 5min period